Materials become insensitive to flaws at nanoscale: Lessons from nature

Huajian Gao[†‡], Baohua Ji[†], Ingomar L. Jäger[§], Eduard Arzt[†], and Peter Fratzl[§]

[†]Max Planck Institute for Metals Research, Heisenbergstrasse 3, D-70569 Stuttgart, Germany; and [§]Erich Schmid Institute of Material Science, Austrian Academy of Sciences and Metal Physics Institute, University of Leoben, Jahnstrasse 12, A-8700, Leoben, Austria

Communicated by Zdenek P. Bazant, Northwestern University, Evanston, IL, March 20, 2003 (received for review September 9, 2002)

Natural materials such as bone, tooth, and nacre are nanocomposites of proteins and minerals with superior strength. Why is the nanometer scale so important to such materials? Can we learn from this to produce superior nanomaterials in the laboratory? These questions motivate the present study where we show that the nanocomposites in nature exhibit a generic mechanical structure in which the nanometer size of mineral particles is selected to ensure optimum strength and maximum tolerance of flaws (robustness). We further show that the widely used engineering concept of stress concentration at flaws is no longer valid for nanomaterial design.

Natural materials, such as shells (1–7), tooth (8, 9), or bone (10–12), exhibit many levels of hierarchical structures from macroscopic to microscopic length scales. Despite these complicated hierarchical structures, we find it most interesting to observe that the smallest building blocks in such materials are generally on the nanometer length scale. Fig. 1 *a* and *d* shows that enamel of tooth is made of long, more or less needle-like crystals ≈15–20 nm thick embedded in soft matrix (8, 13). Fig. 1 *b* and *e* shows that the nanostructure of bone consists of mineral crystal platelets with thickness around a few nanometers embedded in a collagen matrix (12, 14, 15). Fig. 1 *c* and *f* shows the "brick and mortar" structure of nacre where the thickness of the aragonite bricks is around a few hundred nanometers (1, 3, 5). Although it is quite clear that the composite character of these materials plays an important role, one important question remains: Why is the nanometer scale so important? Although the stiffness of biocomposites is similar to that of the mineral constituent, their fracture energy can be several orders of magnitude higher than that of the mineral. Monolithic $CaCO_3$ shows a work of fracture that is ≈3,000 times less than that of the composite shell (nacre) (5). Generally, there is a well defined organization of the components in the composite in the form of interlaced bricks separated by soft layers. Mineral lamellae are separated by glue (protein), which results in high toughness by stress-redistribution and crack-stopping mechanisms (16). Previous researchers have tried to address the mechanism of high toughness of these materials from various points of view including their hierarchical structures (2–4, 17), the effects of mechanical properties of protein on dissipating fracture energy (18), protein–mineral interface roughness (16), and reduction of stress concentration at a crack (19). However, the question of why the elementary structure of biocomposites is on the nanometer length scale remains unclear.

At the most elementary structure level, biocomposites exhibit a generic microstructure consisting of staggered mineral bricks shown in Fig. 2*a*. Jaeger and Fratzl (20) discussed the mineral platelet arrangement in collagen fibril and developed a simple mechanical model to estimate the stiffness of biocomposites. Under an applied tensile stress, the Jaeger–Fratzl model can be schematically represented by Fig. 2*b*, where the mineral platelets carry the tensile load while the protein matrix transfers the load between mineral crystals via shear. The path of load transfer in the composite is thus simplified to a one-dimensional serial spring system consisting of mineral elements (tension) interspersed among protein elements (shear). The large aspect ratio of mineral platelets compensates for the low modulus of the protein phase. According to this simple model, the stiffness (Young's modulus) E of the composite can be expressed as

$$\frac{1}{E} = \frac{4(1-\Phi)}{G_p \Phi^2 \rho^2} + \frac{1}{\Phi E_m}, \qquad [1]$$

where E_m is the Young's modulus of mineral, G_p is the shear modulus of protein, Φ is the volume concentration of mineral, and ρ is the aspect ratio of the mineral platelets (20). We found that Eq. **1** compares very well with finite element calculations. Fig. 2 and Eq. **1** indicate that the high stiffness of biocomposites is achieved by the large aspect ratio of mineral platelets, that

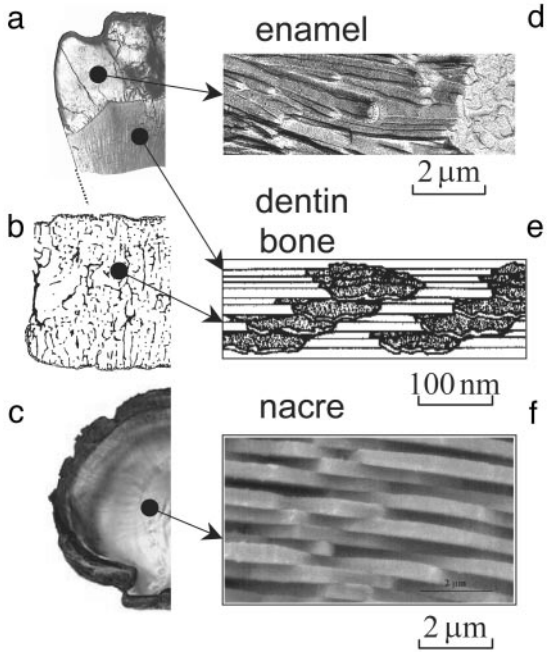

Fig. 1. Many hard biological tissues, such as tooth (*a*), vertebral bone (*b*), or shells (*c*) are made of nanocomposites with hard mineral platelets in a soft (protein) matrix. Enamel (*d*) is made of long, more or less needle-like crystals ≈15–20 nm thick and 1,000 nm long, with a relatively small volume fraction of a soft protein matrix (8, 13). Dentin and bone (*e*) are made up of plate-like crystals (2–4 nm thick, up to 100 nm long) embedded in a (collagen-rich) protein matrix (12, 14, 15). The volume ratio of mineral to matrix is on the order of 1:2. Nacre (*f*) is made of plate-like crystals (200–500 nm thick and a few micrometers long) with a very small amount of soft matrix in between (3). All of the composites share the structural feature of hard platelets with a very large aspect ratio, arranged parallel in a brick-and-mortar-like fashion. An unsolved problem is the question of why these crystals are in the nanometer range.

[‡]To whom correspondence should be addressed. E-mail: hjgao@mf.mpg.de.

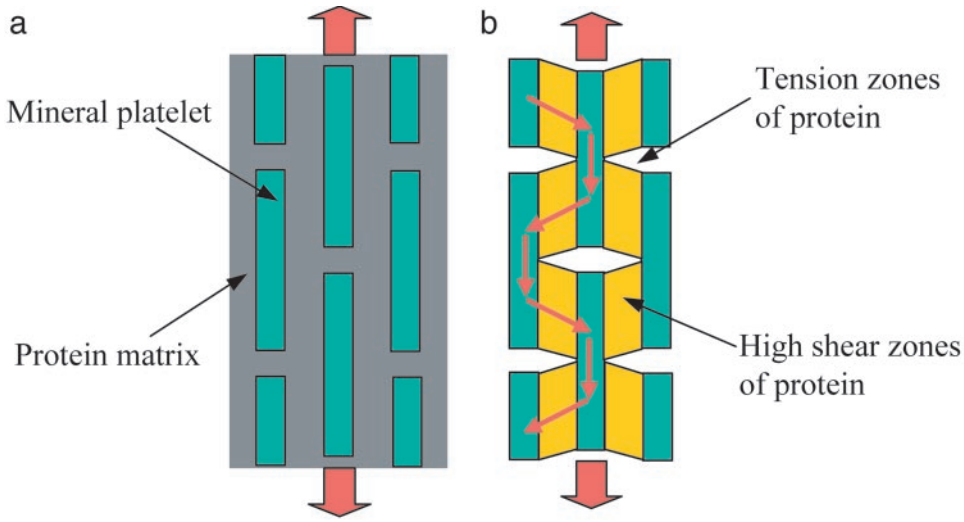

Fig. 2. A model of biocomposites. (*a*) A schematic diagram of staggered mineral crystals embedded in protein matrix. (*b*) A simplified model showing the load-carrying structure of the mineral–protein composites. Most of the load is carried by the mineral platelets whereas the protein transfers load via the high shear zones between mineral platelets.

most of the load is carried by the hard mineral platelets, and that the protein transfers stress between platelets via shear.

To ensure integrity and optimized strength of the composite structure shown in Fig. 2*b*, the mineral platelets must be able to sustain large tensile stress without fracture, whereas the protein layer and protein/mineral interface must sustain shear stress without failure. The fracture toughness of the composite thus hinges on the tensile strength of mineral platelets. How to optimize the strength of mineral platelets? A clue to this question can be obtained from the following consideration. A perfect, defect-free mineral platelet should be able to sustain mechanical stress near the theoretical strength σ_{th} of solid. However, for robust design one must consider the possibility that the mineral platelet actually contains crack-like flaws. What we have in mind as crack-like flaws are protein molecules that have been trapped within the mineral crystals during the biomineralization process. The soft "protein inclusions" within a hard mineral crystal are mechanically equivalent to embedded microcracks due to their low modulus. Consider a thumbnail crack in the mineral platelet as shown in Fig. 3*a*. The fracture strength of this "cracked" mineral platelet can be calculated from the Griffith criterion as

$$\sigma_m^f = \alpha E_m \Psi, \qquad \Psi = \sqrt{\frac{\gamma}{E_m h}}, \qquad [2]$$

where γ is the surface energy and h is the thickness of mineral crystal. The parameter α depends on the crack geometry and is approximately equal to $\sqrt{\pi}$ for the half-cracked platelet (i.e., crack depth equals half of the platelet thickness). Fig. 3*b* compares this result with the strength of a defect-free crystal. We see that there exists a critical length scale

$$h^* \approx \alpha^2 \frac{\gamma E_m}{\sigma_{th}^2} \qquad [3]$$

below which the fracture strength of a cracked crystal is identical to that of a perfect crystal. Taking a rough estimate $\gamma = 1$ J/m^2 (19, 21), $E_m = 100$ GPa, and $\sigma_{th} = E_m/30$, we estimate h^* to be $\approx$30 nm. This length scale indicates that the nanometer size of mineral platelets in biocomposites may be the result of fracture strength optimization. When the mineral size exceeds this length scale, the fracture strength is sensitive to structural size and the

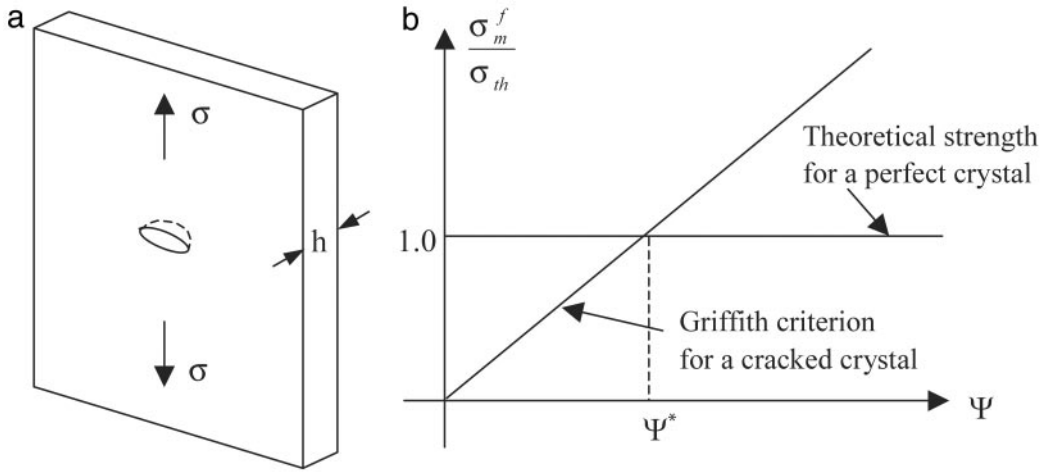

Fig. 3. A length scale for optimized fracture strength in mineral platelet. (*a*) A schematic diagram of mineral platelet with a surface crack. (*b*) Comparison of the fracture strength of a cracked mineral platelet calculated from the Griffith criterion with the strength of a perfect crystal.

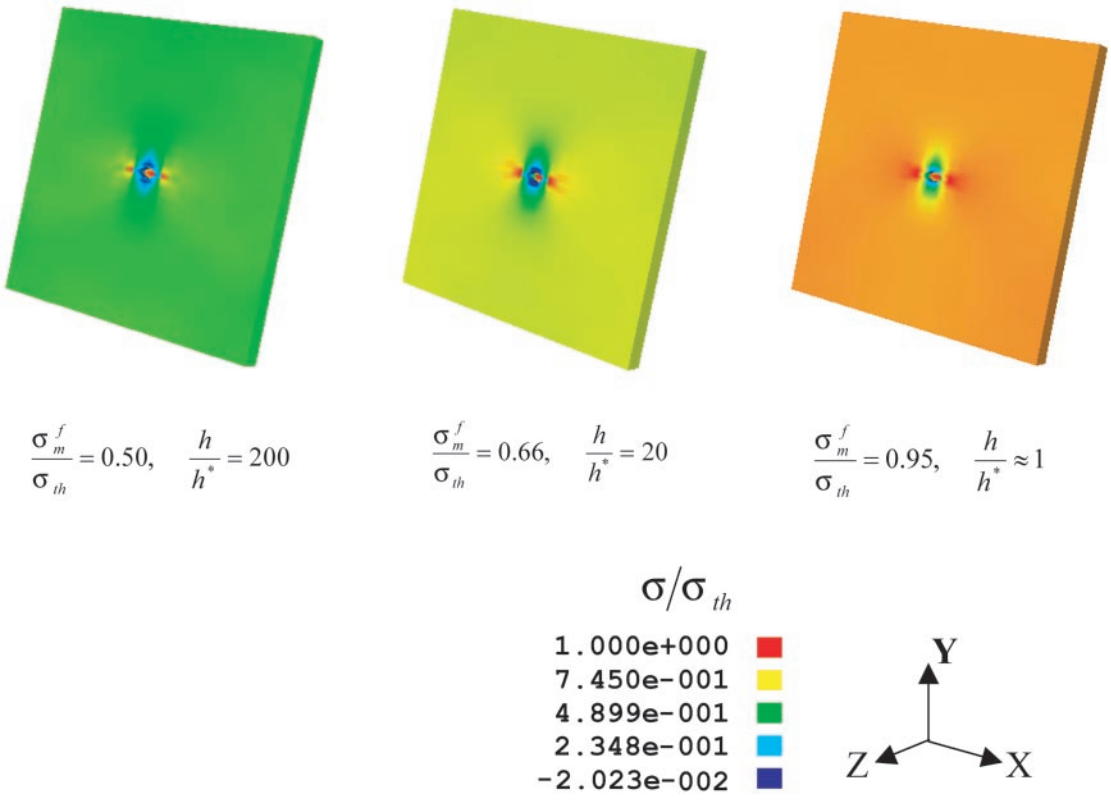

Fig. 4. The color map of normal stress σ_{22} at critical fracture load in a mineral platelet containing a thumbnail crack with depth equal to half of the platelet thickness. The calculation is performed by using a 3D finite element method based on the virtual internal bond model, as the thickness of the mineral platelet decreases toward the critical thickness for optimum fracture strength. At large thicknesses ($h/h^* = 20,200$), the stress concentration at the crack tip significantly reduces the fracture strength σ_f from the theoretical strength σ_{th}. Near the critical thickness h^*, the stress concentration vanishes and the strength approaches the theoretical strength.

material is sensitive to crack-like flaws and fails by stress concentration at crack tips. As the mineral size drops below this length scale, the strength of a perfect mineral platelet is maintained despite defects. The failure criterion is governed by theoretical strength rather than by the Griffith criterion and the material becomes insensitive to preexisting flaws. Therefore, we make the following postulate: The nanometer size of the mineral crystals in biocomposites is selected to ensure optimum fracture strength and maximum tolerance of flaws (for robustness).

The critical length of 30 nm is only a rough estimate representing the objective of unconstrained biological optimization with respect to fracture strength of mineral crystals. One may note that the thickness of mineral platelets in nacre can be several hundred nanometers larger than the estimated value. In our opinion, the thickness of mineral platelets in nacre may be a result of constrained optimization caused by the large volume fractions of mineral content in nacre. For example, at a mineral volume fraction of 95% and a protein layer thickness of 10 nm (which is already approaching the minimum size of single protein molecules), the mineral crystal needs to be of a minimum thickness of 200 nm! This boundary condition results in constrained optimization with respect to fracture strength.

Fracture of solids involves breaking of atomic bonds, which is inherently a nonlinear process. To model failure mechanisms in nanomaterials, we have developed a virtual internal bond (VIB) (22, 23) method, which incorporates an atomic cohesive force law into the constitutive model of materials. Fig. 4 shows the stress field in a surface cracked mineral platelet calculated by a VIB-based finite element analysis as the platelet is loaded close to the failure limit. It shows that the stress field becomes more and more uniform as the thickness of the platelet decreases and eventually reaches the theoretical strength at the critical length scale. This finding is in drastic contrast to the classical engineering concept of stress concentration at macroscopic flaws.

The analysis discussed here also shows that there is an optimum aspect ratio of the mineral platelets

$$\rho^* = \frac{1}{\tau_p^f}\sqrt{\frac{\pi E_m \gamma}{h}}, \qquad [4]$$

where τ_p^f is the shear strength of protein matrix. This equation can be derived as follows. A simple force balance in the nanostructure model shown in Fig. 2 indicates that the tensile stress σ_m in the mineral platelets is equal to the product of the mineral aspect ratio with the shear stress τ_p in the protein matrix, i.e., $\sigma_m = \rho\tau_p$. The optimum aspect ratio corresponds to the condition that protein and mineral fail at the same time, i.e., $\rho^* = \sigma_m^f/\tau_p^f$ (the superscript denotes "failure strength"). Assuming that the mineral strength is governed by the Griffith criterion of Eq. **2** immediately leads to Eq. **4**. We note that a large mineral aspect ratio is required if the mineral strength is much higher than the shear strength of the protein or the protein/mineral interface. Eq. **4** shows that the optimum aspect ratio of mineral platelets is inversely proportional to the square root of the mineral thickness: the smaller the platelets, the larger the optimal aspect ratio; the larger the aspect ratio, the larger the stiffening effect. The mineral crystals in bone have thickness on the order of a few nanometers and aspect ratio 30–40 and those in nacre have thickness on the order of a few hundred

nanometers and aspect ratio ≈10, which roughly corresponds to the scaling law predicted by Eq. **4**.

The question of whether an optimum thickness of protein layer exists between mineral platelets is also very interesting. This would correspond to an optimum volume fraction of mineral content. This question should be answered by a careful study of dynamic failure mechanisms of biocomposites. Our preliminary studies of impact fracture indicated that the soft protein phase plays a key role in alleviating impact damage to mineral platelets and to protein/mineral interfaces. Qualitatively, the protein matrix behaves like a soft wrap around mineral platelets and protects them from the peak stresses caused by impact and homogenizes stress distribution within the composite. The endoskeleton of animals contains much higher protein content and lower mineral concentration than the seashells. According to Eq. **1**, to achieve the same level of stiffening, a lower volume fraction Φ must be compensated for by a large aspect ratio ρ, and larger aspect ratio means smaller thickness. This explains why the mineral platelets in human bone have much smaller size and larger aspect ratios in comparison with those found in seashells.

We note that the bio-inspired length scale for optimum platelet strength

$$\gamma E_m/\sigma_{th}^2 \qquad \textbf{[5]}$$

is an intrinsic material parameter that measures the size of fracture process zone in a brittle material. The major conclusion of this investigation is that materials become insensitive to flaws as soon as the structural size reaches this critical length. This result should be of general significance in guiding design of new nanomaterials. Also, hierarchical laminated structures are needed to produce materials capable of sustaining more complex mechanical stresses. Future research should be directed at understanding the coupling between different levels of hierarchical structures.

As a final note, we want to point out some limitations of our simple analysis. Although we have emphasized the overarching importance of mechanical strength as a fundamental driving force for nanostructural optimization in biological materials, such optimization in individual biosystems can be subjected to many other constraints, including stoichiometric conditions and chemical factors that could affect the size of mineral crystals (24, 25). We have already mentioned the constraint caused by mineral volume fraction and minimum size of protein molecules. These factors play important roles in the nucleation and formation of mineral crystals and lead to constrained optimization of biosystems. Our analysis has only emphasized that there may be an overarching driving force of a scale selection motivated by mechanical strength considerations and, as such, it does not diminish in any sense the important roles of the chemical environment in the biomineralization process.

This work was supported by the Max Planck Society, the National Science Foundation of China, and the Cheung Kong Scholar program through Tsinghua University.

1. Currey, J. D. (1977) *Proc. R. Soc. London Ser. B* **196,** 443–463.
2. Menig, R., Meyers, M. H., Meyers, M. A. & Vecchio, K. S. (2001) *Mater. Sci. Eng.* **297**, 203–211.
3. Menig, R., Meyers, M. H., Meyers, M. A. & Vecchio, K. S. (2000) *Acta Mater.* **48,** 2383–2398.
4. Kamat, S., Su, X., Ballarini, R. & Heuer, A. H. (2000) *Nature* **405,** 1036–1040.
5. Jackson, A. P., Vincent, J. F. V. & Turner, R. M. (1988) *Proc. R. Soc. London Ser. B* **234,** 415–440.
6. Taylor, J. D. (1973) *Palaeontology* **16,** 519–534.
7. Currey, J. D. & Taylor, J. D. (1974) *J. Zool. (London)* **173,** 395–406.
8. Tesch, W., Eidelman, N., Roschger, P., Goldenberg, F., Klaushofer, K. & Fratzl, P. (2001) *Calcif. Tissue Int.* **69,** 147–157.
9. Weiner, S., Veis, A., Beniash, E., Arad, T., Dillon, J. W., Sabsay, B. & Siddiqui, F. (1999) *J. Struct. Biol.* **126,** 27–41.
10. Rho, J. Y., Kuhn-Spearing, L. & Zioupos, P. (1998) *Med. Eng. Phys.* **20,** 92–102.
11. Weiner, S. & Wagner, H. D. (1998) *Annu. Rev. Mater. Sci.* **28,** 271–298.
12. Landis, W. J. (1995) *Bone* **16,** 533–544.
13. Warshawsky, H. (1989) *Anat. Rec.* **224,** 242–262.
14. Landis, W. J. & Hodgens, K. J. (1996) *J. Struct. Biol.* **117,** 24–35.
15. Roschger, P., Grabner, B. M., Rinnerthaler, S., Tesch, W., Kneissel, M., Berzlanovich, A., Klaushofer, K. & Fratzl, P. (2001) *J. Struct. Biol.* **136,** 126–136.
16. Wang, R. Z., Suo, Z., Evans, A. G., Yao, N. & Aksay, I. A. (2001) *J. Mater. Res.* **16,** 2485–2493.
17. Kessler, H., Ballarini, R., Mullen, R. L., Kuhn, L. T. & Heuer, A. H. (1996) *Comput. Mater. Sci.* **5,** 157–166.
18. Smith, B. L., Schaeffer, T. E., Viani, M., Thompson, J. B., Frederick, N. A., Kindt, J., Belcher, A., Stucky, G. D., Morse, D. E. & Hansma, P. K. (1999) *Nature* **399**, 761–763.
19. Okumura, K. & de Gennes, P.-G. (2001) *Eur. Phys. J. E* **4,** 121–127.
20. Jaeger, I. & Fratzl, P. (2000) *Biophys. J.* **79,** 1737–1746.
21. Gilman, J. J. (1960) *J. Appl. Phys.* **31,** 2208–2218.
22. Gao, H. & Klein, P. A. (1998) *J. Mech. Phys. Solids* **46,** 187–218.
23. Klein, P. A., Foulk, J. W., Chen, E. P., Wimmer, S. A. & Gao, H. (2001) *Theor. Appl. Fract. Mech.* **37,** 99–166.
24. Glimcher, M. J. (1984) *Philos. Trans. R. Soc. London B* **304,** 479–508.
25. Hunter, G. K., Hauschka, P. V., Poole, A. R., Rosenberg, L. C. & Goldberg, H. A. (1996) *Biochem. J.* **317,** 59–64.